

Magnetoelectric Mapping as Observed in Quantum Coherence Phenomena under Strong Spin-Orbit Interaction

J. J. HEREMANS,^{1,*} R. L. KALLAHER,¹ M. RUDOLPH,¹
AND M. B. SANTOS²

¹Department of Physics, Virginia Tech, Blacksburg, VA 24061, USA

²Homer L. Dodge Department of Physics and Astronomy, University of Oklahoma, Norman, OK 73019, USA

A magnetoelectric mapping is demonstrated between dephasing effects of the magnetic vector potential and effects of an effective vector potential describing spin-orbit interaction. The experiments use spin-dependent mesoscopic quantum transport experiments on the narrow-gap semiconductor InSb and the semimetal Bi, both materials with strong spin-orbit interaction. The spin-orbit-induced antilocalization signature in transport allows determination of spin coherence lengths in narrow InSb and Bi wires. Spin coherence lengths are observed to increase with decreasing wire widths. The geometrical effect of width can be understood from the magnetoelectric duality between the Aharonov-Bohm phase and the Aharonov-Casher phase.

Keywords Spin-orbit interaction; spin coherence; quantum coherence; Aharonov-Casher phase; Aharonov-Bohm phase; magnetoelectric phenomena

Spin-orbit interaction (SOI) in materials inspires the creation of effective gauge fields, and can lead to new quantum states of matter constructed in analogy to quantum states at high magnetic fields. Materials with strong SOI include the narrow-bandgap semiconductor InSb and the semimetal bismuth, and are the focus of the present work. Spin-dependent mesoscopic quantum transport experiments in submicron wires nanolithographically fabricated from InSb and Bi epitaxial materials [1,2] show that the spin coherence lengths L_{so} increase with decreasing wire widths w if other parameters stay constant. Other experiments [3–8], as well as theoretical work [9] also indicate that L_{so} lengthens as w narrows, and this finding has positive implications for nanoscaled spintronics. The emphasis of the present work lies in showing that the result can be approached using the magnetoelectric duality between the Aharonov-Bohm (AB) [10] phase under magnetic fields B and the Aharonov-Casher (AC) [11–14] phase under SOI, and using a geometrical argument relying on the accumulation of a Berry's phase. Such magnetoelectric mapping between the physics of solid-state systems under magnetic fields on one hand and under SOI on the other hand, could in fact be extended to other dephasing phenomena induced by various Berry's phase occurrences. As

Received in final form June 13, 2015.

*Corresponding author. E-mail: heremans@vt.edu

Color versions of one or more of the figures in the article can be found online at www.tandfonline.com/gin.

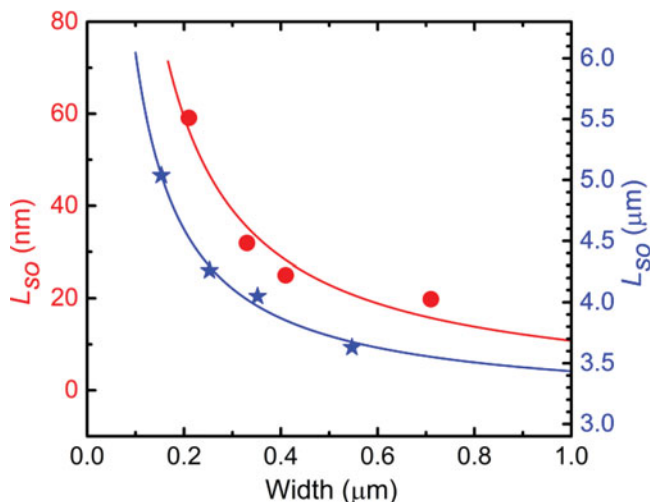


Figure 1. Experimental values of L_{so} vs wire width for Bi wires (red circles, left-hand scale) and InSb quantum well wires (blue stars, right-hand scale), obtained at 0.39 K. Lines are fits to a $1/\text{width}$ dependence.

a corollary, the lengthening of L_{so} in narrow Bi wires is consistent with Bi having surface states with strong Rashba-like SOI [2,15–17].

The method used to quantify L_{so} , together with the quantum phase coherence length L_{ϕ} , is antilocalization (AL). The AL phenomenon originates in a quantum correction to the magnetoresistance resulting from electron interference on time-reversed closed trajectories in the material. As a quantum interference experiment AL can be used to measure quantum coherence lengths, including L_{so} [9,18–20], using low-temperature magnetoresistance measurements. The magnetoresistance is characterized for sets of parallel wires at low temperatures $T \approx 0.39$ K and at low B applied perpendicularly to the plane of the heterostructure or thin film samples. The wires are in the quasi-one-dimensional (Q1D) regime, where w , L_{so} , L_{ϕ} and the elastic mean-free-path l_e are all comparable. The analysis therefore uses a Q1D AL theory [1,8,21], which allows quantitative determination [19–22] of L_{so} and L_{ϕ} as obtained from a fit of the experimental wire conductance $G(B)$ to theory. Measured is the change in resistance $R = 1/G$ under applied B , whereas AL theory models $\Delta G = G(B) - G(B = 0)$. Yet using the measured $\Delta R = R(B) - R(0)$ and realizing that $\Delta R/R^2 \approx -\Delta G$, theory and experiment can be fitted.

Wires of different width were fabricated on Bi(111) (rhombohedral notation) thin films and on InSb/InAlSb heterostructures, using electron-beam lithography and wet and reactive ion etching, respectively. Bi(111) thin films were thermally evaporated from a Bi (99.999%) source onto SiO₂ (oxidized Si(001)) substrate [2,23]. Bi film growth of thickness 75 nm [23], resulted in a trigonal axis perpendicular to the substrate [24], with grains of size 200–500 nm randomly oriented, such that the Bi(111) trigonal face was exposed. The films showed compensated electron and hole densities, $\sim 2 \times 10^{24} \text{ m}^{-3}$ indicative of high-quality Bi (mobilities $\sim 0.1 \text{ m}^2/\text{Vs}$). However, the AL measurements were dominated by the surface carriers of Bi(111) [15–17], particularly from the surface electron pocket. Wires of length $L = 16 \mu\text{m}$ were fabricated on the Bi(111) thin films. The InSb quantum well of thickness 25 nm was contained in a In_{0.85}Al_{0.15}Sb/InSb/In_{0.85}Al_{0.15}Sb heterostructure [1] grown by molecular beam epitaxy on (001) GaAs substrates. The unpatterned heterostructure showed

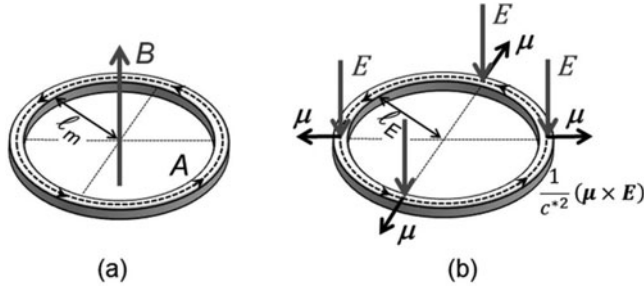


Figure 2. (a) Schematic representation of a closed path of a charge in magnetic field B , where the accumulated Aharonov-Bohm phase equals π if the average radius equals the magnetic length l_m . The vector potential A is indicated on the circumference. (b) Schematic representation of a closed path of a magnetic moment μ in electric field E , where the accumulated Aharonov-Casher phase equals π if the average radius equals the electric length l_E . The AC vector potential A_{ac} is indicated on the circumference.

at 0.39 K an areal carrier density $5.2 \times 10^{15} \text{ m}^{-2}$ with mobility $9.7 \text{ m}^2/\text{Vs}$. Wires of length $L = 24 \mu\text{m}$ were fabricated on this heterostructure. Figure 1 shows data for L_{so} vs w for Bi and InSb wires, obtained at $T = 0.39 \text{ K}$ [1,21]. The values for L_{so} were extracted using the method described below. Of importance in this work, L_{so} shows an approximate dependence $L_{so} \sim 1/w$ (fitted lines in Fig. 1) which will be discussed below.

The characteristic path length for accumulation of a quantum phase plays an important role in limiting the length over which a wave packet retains coherence. Experimental situations do not distinguish between dephasing due to effective or actual gauge fields, in principle a reversible process, and decoherence due to interactions with the environment, which is not reversible. The Q1D model of AL, described below, illustrates how the effects of an accumulated quantum AB phase (effect of B on charge e) or an accumulated quantum AC phase [11–14] under SOI (effect of electric field E on magnetic moment μ), add to the intrinsic decoherence phenomena described by L_ϕ , to limit the effective phase coherence length. We will call this effective phase coherence length L_{eff} .

In a system of length L and width w at $B = 0$ and without SOI, the quantum correction (per spin channel) to the 2-dimensional conductivity $\sigma_{2D} = (L/w)G$ depends on L_{eff} as follows [25,26]:

$$\delta\sigma_{2D} = -\frac{1}{2} \frac{e^2}{\pi\hbar} \frac{L_{eff}}{w} \quad (1)$$

The AB phase [10] $\Delta\phi_{AB}$ accumulated over a closed path length,

$$\Delta\phi_{AB} = \frac{1}{\hbar} \oint e A \times dl \quad (2)$$

leads to dephasing over the time-reversed closed trajectories leading to AL, a time-reversal symmetry breaking effect. Here A is the magnetic vector potential associated with B , and the line element dl is to be taken over the path. A closed path of average radius $l_m \equiv (\hbar/eB)^{1/2}$ encloses a magnetic flux $\pi(\hbar/e)$ and a particle with charge e over such path will accumulate a quantum phase of π . A schematic geometric construction of such closed path is illustrated in Fig. 2a. The magnetic length l_m is thus a characteristic length for AB dephasing. In the presence of perpendicular B , and if $l_m < w$, the phase coherence length L_ϕ can be seen to

be reduced to $L_{\text{eff}} = (L_\phi^{-2} + l_m^{-2})^{-1/2}$, and the B -dependence of the quantum correction $\delta\sigma_{2D}(B)$ is carried by l_m . If we now introduce SOI, L_ϕ is further replaced in Eq. 1 by singlet and triplet lengths [1,8,9,19,21,25,27,28] originating in pairing of the two time-reversed trajectories (Cooperons). The singlet length $L_{0,0}$ is unaffected by SOI [1,8,21,28] and hence $L_{0,0} = (L_\phi^{-2} + l_m^{-2})^{-1/2}$, while the triplet lengths are $L_{1,\pm 1} = (L_\phi^{-2} + L_{so}^{-2} + l_m^{-2})^{-1/2}$ and $L_{1,0} = (L_\phi^{-2} + 2L_{so}^{-2} + l_m^{-2})^{-1/2}$. In Eq. 1, we then have $L_{\text{eff}} = (L_{1,1} + L_{1,-1} + L_{1,0} - L_{0,0})$. Using $(w/L) \delta\sigma_{2D}(B) = \delta G(B)$, where $\delta G(B) = G(B) - G_0$ and where G_0 is the classical conductance at $B = 0$, and using $\Delta R/R^2 \approx -\Delta G = -(G(B) - G(B=0)) = -(\delta G(B) - \delta G(B=0))$, the experimental data can be fitted to Eq.1 to obtain L_{so} and L_ϕ . For a proper fit to wires of finite L and to take into account ballistic effects, some corrections [1,8,21,29,30] have to be applied to L_{eff} but these corrections don't alter the discussion below centered on the observation that L_{so} increases with narrowing w (Fig. 1).

The increase of L_{so} in narrow wires (Fig. 1) can be understood via the use of an effective SOI vector potential, in analogy to the magnetic case. Linear Rashba-type SOI [31] resulting from a unidirectional breaking of spatial inversion symmetry can be mapped on the physics arising from an effective vector potential [32], namely $\mathbf{A}_{ac} = (1/c^{*2})(\boldsymbol{\mu} \times \mathbf{E})$, with $\boldsymbol{\mu}$ the particle's magnetic moment, \mathbf{E} the (uniform) effective or actual electric field breaking inversion symmetry and thereby resulting in SOI, and c^* the effective velocity of light (a bandstructure parameter, as in Ref. 33). We call \mathbf{A}_{ac} the Aharonov-Casher vector potential, and it gives rise to an AC phase [11-13] $\Delta\phi_{AC}$, analogously to the magnetic \mathbf{A} giving rise to the AB phase (Eq. 2):

$$\Delta\phi_{AC} = \frac{1}{\hbar} \oint \frac{1}{c^{*2}} (\boldsymbol{\mu} \times \mathbf{E}) \cdot d\mathbf{l} \quad (3)$$

The AB and AC phase are magnetolectric duals, with the AB phase describing the effect of B on charge e and the AC phase describing the effect of \mathbf{E} on magnetic moment $\boldsymbol{\mu}$. In analogy to Fig. 2a, Fig. 2b shows a closed path geometry where the uniform \mathbf{E} is perpendicular to the path as expected for heterostructures or Bi thin films, and $\boldsymbol{\mu}$ is perpendicular to both \mathbf{E} and the path elements (the alignment for the lowest energy state). In Fig. 2b, a closed path of average radius $l_E \equiv \hbar c^{*2}/(2E\boldsymbol{\mu})$ circumscribes $\pi(\hbar/\boldsymbol{\mu})$ and a particle with magnetic moment $\boldsymbol{\mu}$ over such path will accumulate a quantum phase of π . The electric length l_E is thus a characteristic length for AC dephasing, fulfilling a role dual to l_m . Insight in the nature of l_E can be obtained by using the mapping to linear Rashba SOI. For particles of spin 1/2, we have $\boldsymbol{\mu} = 1/2 \mu_B$ with μ_B the Bohr magneton. Then the Hamiltonian containing \mathbf{A}_{ac} maps on the Hamiltonian for linear Rashba SOI [32] with Rashba parameter $\alpha = E \hbar^2 e/(4m^{*2} c^{*2})$, where m^* is the effective mass at the band edge. The zero- B energy splitting under linear Rashba SOI [31] is $\hbar\Omega = 2k_F\alpha$ (with k_F the Fermi wavevector), defining the spin precession frequency Ω due to SOI. The spin precession length is then determined as $L_\Omega = v_F/\Omega$ with v_F the Fermi velocity, and for a parabolic dispersion [9,34] we obtain $L_\Omega = \hbar^2/(2 m^*\alpha)$. Under the D'yakanov-Perel' (DP) motional narrowing spin decoherence mechanism assuming linear Rashba SOI (or linear Dresselhaus SOI) [3,9,20,34], the spin decoherence rate $1/\tau_{so} = \Omega^2 \tau_e/2$, with τ_e the momentum relaxation time such that $l_e = v_F\tau_e$. With the two-dimensional diffusion coefficient $D = v_F^2\tau_e/2$, we obtain $L_{so} = (D\tau_{so})^{1/2} = L_\Omega$. Using the expression for α , we further find $l_E \equiv \hbar c^{*2}/(2E\boldsymbol{\mu}) = \hbar^2/(2 m^*\alpha) = L_\Omega = L_{so}$. Hence, under DP spin decoherence and linear Rashba SOI, the electric length l_E yielding an AC phase of π over a closed loop, equals the spin coherence length L_{so} . This equality quantitatively confirms the dephasing

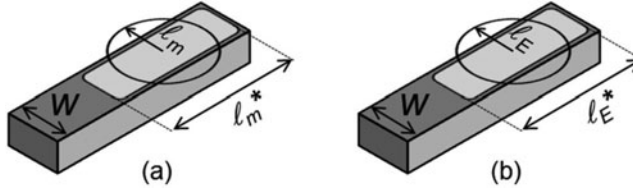


Figure 3. (a) Schematic representation of the geometrical constraint on magnetic flux accumulation and hence Aharonov-Bohm phase accumulation in a wire of width $w < l_m$. The effective magnetic length has to stretch to l_m^* . (b) Schematic representation of the geometrical constraint on line-integral (Eq. 3) accumulation and hence Aharonov-Casher phase accumulation in a wire of width $w < l_E$. The effective electric length has to stretch to l_E^* .

influence of \mathbf{A}_{ac} in analogy to the magnetic \mathbf{A} and establishes the magnetoelectric duality between the coherence-limiting roles of l_m and l_E .

Figure 3a illustrates that if in a two-dimensional system the closed path accumulating an AB phase (Eq. 2) is constrained in a narrow wire to $w < l_m$ along one direction, then acquiring the same AB phase will require the particle traveling over distance $l_m^* \approx \pi l_m^2/w$ in the orthogonal direction to enclose the *same area*. The proportionality of the AB phase to the area enclosed by the path (and enclosed magnetic flux) is a consequence of Stokes' theorem and the fact that $\mathbf{B} = \nabla \times \mathbf{A}$ (related to gauge invariance). The length l_m^* becomes the effective free length for dephasing. From this geometrical interpretation, we expect $l_m^* \sim l_m^2/w$ in narrow wires. A more detailed calculation [25,29] considering the modification due to boundary conditions of the Landau basis for wave functions constrained to a wire finds that $l_m^* = 3^{1/2} l_m^2/w$, consistent with the geometrical approach. Since $l_m^* > l_m$, a narrow wire will delay AB dephasing to higher B , or effectively lower the influence of B in L_{eff} . This effect is indeed observed in AL experiments [1,8].

The observation that L_{so} increases for narrowing w (Fig. 1) can now be understood via the duality between the roles of l_m and l_E and via $l_E = L_{so}$. Figure 3b illustrates that if a closed path, now accumulating an AC phase (Eq. 3), is constrained in a narrow wire to $w < l_E$, then acquiring the same AC phase will require that the particle travel over distance l_E^* along the wire, such that $2\pi l_E = 2w + 2l_E^*$ to circumscribe the *same path length*. A proportionality to enclosed area or to a flux via Stokes' theorem can indeed not be achieved for the AC phase for uniform \mathbf{E} . We expect $L_{so} = l_E^* \approx \pi l_E - w$. Thus, the geometrical interpretation of accumulated AC phase predicts that L_{so} increases for narrowing w , as observed experimentally. But $L_{so} \sim 1/w$ [9] is not strictly recovered, since the AC phase is acquired over a path length rather than over an area like the AB phase. The experimental data for L_{so} vs w presented in Fig. 1 and in other literature [3-8] is at present not sufficiently precise to determine whether $L_{so} \sim 1/w$ is in fact strictly followed, and the data is hence judged compatible with the geometrical interpretation of accumulated AC phase. Future experiments will be aimed at verifying whether an algebraic dependence $L_{so} \approx \pi l_E - w$ forms a better fit to the data, and at verifying the prefactors. Both the data and the geometrical model however agree that in a narrow wire AC dephasing and hence equivalently spin decoherence due to SOI will be suppressed, a finding of scientific and technological value.

In conclusion, low-temperature spin coherence lengths in mesoscopic wires of the strongly spin-orbit coupled materials InSb and Bi were obtained by antilocalization measurements. It is observed that the spin coherence lengths increase as the wire widths

decrease, consistent with the literature. The suppression of spin decoherence is validated by use of the magnetoelectric duality between the Aharonov-Bohm and Aharonov-Casher phases and by use of a geometrical approach to describe dephasing due to the accumulation of Berry's phases.

Funding

The work was supported by the U.S. Department of Energy, Office of Basic Energy Sciences, Division of Materials Sciences and Engineering under award DOE DE-FG02-08ER46532 (JJH), and by the National Science Foundation under award DMR-0520550 (MBS).

References

1. R. L. Kallaher, J. J. Heremans, N. Goel, S. J. Chung, and M. B. Santos, "Spin and phase coherence lengths in n-InSb quasi-one-dimensional wires," *Phys. Rev. B* **81**, 035335 (1–7) (2010).
2. M. Rudolph and J. J. Heremans, "Spin-orbit interaction and phase coherence in lithographically defined bismuth wires," *Phys. Rev. B* **83**, 205410 (1–6) (2011).
3. A. W. Holleitner, V. Sih, R. C. Myers, A. C. Gossard, and D. D. Awschalom, "Suppression of spin relaxation in submicron InGaAs wires," *Phys. Rev. Lett.* **97**, 036805 (1–4) (2006).
4. T. Schaeper, V. A. Guzenko, M. G. Pala, U. Zuelicke, M. Governale, J. Knobbe, and H. Hardtdegen, "Suppression of weak antilocalization in GaInAs/InP narrow quantum wires," *Phys. Rev. B* **74**, 081301(R) (1–4) (2006).
5. Y. Kunihashi, M. Kohda, and J. Nitta, "Enhancement of spin lifetime in gate-fitted InGaAs narrow wires," *Phys. Rev. Lett.* **102**, 226601 (1–4) (2009).
6. D. Liang, J. Du, and X. Gao, "Anisotropic magnetoconductance of a InAs nanowire: angle dependent suppression of one-dimensional weak localization," *Phys. Rev. B* **81**, 153304 (1–4) (2010).
7. P. Roulleau, T. Choi, S. Riedi, T. Heinzl, I. Shorubalko, T. Ihn, and K. Ensslin, "Suppression of weak antilocalization in InAs nanowires," *Phys. Rev. B* **81**, 155449 (1–4) (2010).
8. R. L. Kallaher, J. J. Heremans, W. V. Roy, and G. Borghs, "Spin and phase coherence lengths in InAs wires with diffusive boundary scattering," *Phys. Rev. B* **88**, 205407 (1–7) (2013).
9. S. Kettemann, "Dimensional control of antilocalization and spin relaxation in quantum wires," *Phys. Rev. Lett.* **98**, 176808 (1–4) (2007).
10. Y. Aharonov and D. Bohm, "Significance of electromagnetic potentials in quantum theory," *Phys. Rev.* **115**, 485–491 (1959).
11. Y. Aharonov and A. Casher, "Topological quantum effects for neutral particles," *Phys. Rev. Lett.* **53**, 319–321 (1984).
12. J. Anandan, "Classical and quantum interaction of the dipole," *Phys. Rev. Lett.* **85**, 1354–1357 (2000).
13. L. L. Xu, S. Ren, and J. J. Heremans, "Magnetoelectronics at edges in semiconductor structures: helical Aharonov-Casher edge states," *Integr. Ferroelectr.* **131**, 36–46 (2011).
14. H. Mathur, and D. Stone, "Quantum transport and the electronic Aharonov-Casher effect," *Phys. Rev. Lett.* **68**, 2964–2967 (1992).
15. P. Hofmann, "The surfaces of bismuth: Structural and electronic properties," *Prog. Surf. Sci.* **81**, 191–245 (2006).
16. T. Hirahara, K. Miyamoto, I. Matsuda, T. Kadono, A. Kimura, T. Nagao, G. Bihlmayer, E. V. Chulkov, S. Qiao, K. Shimada, H. Namatane, M. Taniguchi, and S. Hasegawa, "Direct observation of spin splitting in bismuth surface states," *Phys. Rev. B* **76**, 153305 (1–4) (2007).
17. E. V. C. Yu, M. Koroteev, G. Bihlmayer and S. Bluegel, "First-principles investigation of structural and electronic properties of ultrathin Bi films," *Phys. Rev. B* **77**, 045428 (1–7) (2008).
18. G. Bergmann, "Weak-localization in thin films, a time-of-flight experiment with conduction electrons," *Phys. Rep.* **107**, 1–58 (1984).

19. S. Hikami, A. I. Larkin, and Y. Nagaoka, "Spin-orbit interaction and magnetoresistance in the two dimensional random systems," *Prog. Theor. Phys.* **63**, 707–710 (1980).
20. S. V. Iordanskii, Y. B. Lyanda-Geller, and G. E. Pikus, "Weak localization in quantum wells with spin-orbit interaction," *JETP Lett.* **60**, 206–211 (1994).
21. J. J. Heremans, R. L. Kallaher, M. Rudolph, M. B. Santos, W. Van Roy, and G. Borghs, "Spin-orbit interaction and spin coherence in narrow-gap semiconductor and semimetal wires", *Proc. of the SPIE* **9167**, 91670-D (1–9) (2014).
22. S. McPhail, C. E. Yasin, A. R. Hamilton, M. Y. Simmons, E. H. Linfield, M. Pepper, and D. A. Ritchie, "Weak localization in high-quality two-dimensional systems," *Phys. Rev. B* **70**, 245311 (1–16) (2004).
23. M. Rudolph and J. J. Heremans, "Electronic and quantum phase coherence properties of bismuth thin films," *Appl. Phys. Lett.* **100**, 241601 (1–4) (2012).
24. B. Hackens, J. P. Minet, S. Faniel, G. Farhi, C. Gustin, J. P. Issi, J. P. Heremans, and V. Bayot, "Quantum transport, anomalous dephasing, and spin-orbit coupling in an open ballistic bismuth nanocavity," *Phys. Rev. B* **67**, 121403(R) (1–4) (2003).
25. J. C. Licini, G. J. Dolan, and D. J. Bishop, "Weakly localized behavior in quasi-one-dimensional Li films," *Phys. Rev. B* **54**, 1585–1588 (1985).
26. K. K. Choi, D. C. Tsui, and K. Alavi, "Dephasing time and one-dimensional localization of two-dimensional electrons in GaAs/AlGaAs heterostructures," *Phys. Rev. B* **36**, 7751–7754 (1987).
27. G. J. Dolan, J. C. Licini, and D. J. Bishop, "Quantum interference in lithium ring arrays," *Phys. Rev. Lett.* **56**, 1493–1496 (1986).
28. A. Zduniak, M. Dyakonov, and W. Knap, "Universal behavior of magnetoconductance due to weak localization in two dimensions," *Phys. Rev. B* **56**, 1996–2003 (1997).
29. C. W. J. Beenakker and H. van Houten, "Boundary scattering and weak localization of electrons in a magnetic field," *Phys. Rev. B* **38**, 3232–3240 (1988).
30. M. Ferrier, A. C. H. Rowe, S. Gueron, H. Bouchiat, C. Texier, and G. Montambaux, "Geometrical dependence of decoherence by electronic interactions in a GaAs/AlGaAs square network," *Phys. Rev. Lett.* **100**, 146802 (1–4) (2008).
31. R. Winkler, *Spin-orbit coupling effects in two-dimensional electron and hole systems*, Springer Tracts in Modern Physics 191, Springer-Verlag, Berlin Heidelberg (2003).
32. T. Fujita, M. B. A. Jalil, S. G. Tan, and S. Murakami, "Gauge fields in spintronics," *J. Appl. Phys.* **110**, 121301 (1–29) (2011).
33. W. Zawadzki, "Zitterbewegung and its effects on electrons in semiconductors," *Phys. Rev. B* **72**, 085217 (1–4) (2005).
34. T. Koga, J. Nitta, T. Akazaki, and H. Takayanagi, "Rashba spin-orbit coupling probed by the weak antilocalization analysis in InAlAs/InGaAs/InAlAs quantum wells as a function of quantum well asymmetry," *Phys. Rev. Lett.* **89**, 046801 (1–4) (2002).